Thermal behaviour, surface properties and vibrational spectroscopic studies of the synthesized Co 3x Ni 3À3x (PO 4) 2 $8H 2 O (0 x 1)

ARTICLE · SEPTEMBER 2013

DOI: 10.1016/j.solidstatesciences.2013.07.005

4 AUTHORS:

Saifon Kullyakool
Khon Kaen University
4 PUBLICATIONS **4** CITATIONS
SEE PROFILE

Chanaiporn Danvirutai
Khon Kaen University
40 PUBLICATIONS **371** CITATIONS
SEE PROFILE

Khatcharin Siriwong
Khon Kaen University
25 PUBLICATIONS **348** CITATIONS
SEE PROFILE

Pittayagorn Noisong
Khon Kaen University
15 PUBLICATIONS **91** CITATIONS
SEE PROFILE

Solid State Sciences 24 (2013) 147–153

Contents lists available at ScienceDirect

Solid State Sciences

journal homepage: www.elsevier.com/locate/ssscie

Thermal behaviour, surface properties and vibrational spectroscopic studies of the synthesized $Co_{3x}Ni_{3-3x}(PO_4)_2 \cdot 8H_2O$ ($0 \leq x \leq 1$)

Saifon Kullyakool [a,b], Chanaiporn Danvirutai [a,b,*], Khatcharin Siriwong [c], Pittayagorn Noisong [c]

[a] Materials Chemistry Research Unit, Department of Chemistry and Center for Innovation in Chemistry, Khon Kaen University, Khon Kaen 40002, Thailand
[b] Faculty of Science, Advanced Functional Material Research Cluster, Khon Kaen University, Khon Kaen 40002, Thailand
[c] Materials Chemistry Research Unit, Department of Chemistry, Faculty of Science, Khon Kaen University, Khon Kaen 40002, Thailand

ARTICLE INFO

Article history:
Received 19 May 2013
Received in revised form
2 July 2013
Accepted 3 July 2013
Available online 19 July 2013

Keywords:
Tri(cobalt nickel) diphosphate octahydrate
Thermal properties
Vibrational spectroscopy
Simple synthesis at low temperature
Surface properties

ABSTRACT

$Co_{3x}Ni_{3-3x}(PO_4)_2 \cdot 8H_2O$ ($x = 1$, 0.8, 0.6, 0.4, 0.2, and 0) were synthesized via simple wet chemical reaction and energy saving route method. The final decomposition products of hydrates are corresponding anhydrous tri(cobalt nickel) diphosphates. The metal and water contents of the synthesized hydrates were confirmed by AAS and TG/DTG/DTA techniques, respectively. The observed metal and water contents agree well with the formula of the title compounds. The crystal structures and lattice parameters as well as crystallite sizes of the studied compounds were determined using XRD data. The results from XRD and TG/DTG/DTA techniques confirmed that $Co_{3x}Ni_{3-3x}(PO_4)_2 \cdot 8H_2O$ at all ratios were the single phase. The FTIR spectra of studied compounds were recorded and assigned. The thermal behaviours of single and binary tri(cobalt nickel) diphosphate octahydrates were studied for the first time. The morphologies of the studied compounds were investigated by using the SEM technique. The micrographs of all studied compounds exhibited the thin plated morphology. The surface area and the pore size data of anhydrous forms were measured by N_2 adsorption at −190 °C according to the BET method. The anhydrous forms of binary metal phosphate at $x = 0.8$, $Co_{2.4}Ni_{0.6}(PO_4)_2$, exhibits the highest surface area and expects to improve the catalytic activity.

1. Introduction

Divalent cation phosphates were extensively studied due to their potential applications in industries of various fields such as ceramic dyes and pigments [1–5], catalysts [6–9], bioceramic materials [10], magnetic materials [11,12] and corrosion-protecting materials [13,14]. Specifically, divalent cations such as Co^{2+}, Ni^{2+}, Fe^{2+}, Cu^{2+}, Mn^{2+}, Zn^{2+}, Mg^{2+} and Ca^{2+} phosphates have been used in diverse applications. The mesoporous nickel and cobalt phosphates are the catalysts for styrene oxidation reaction and used as pigments because of their water insoluble and chemically stable properties [1,5,8,9]. They are the catalysts for different organic synthesis reactions [1,8,9], e.g. $Co_3(PO_4)_2$ and $Mg_3(PO_4)_2$. Moreover, $Zn_3(PO_4)_2$ compounds either orthorhombic hopeite or triclinic parahopeite polymorphs are used in coating on steel for corrosive protection [13]. Additionally, calcium phosphates (hydroxyapatite, HA and β-tricalciumphosphate, β-TCP) are found in living bone. They are biomaterials and used as a scaffold of cultured bone and bone graft material [10,15,16] as well as in drug delivery systems [17]. The substitution of different cations has been performed for development of surface [18–20], catalytic activity [21–24], colour [25,26] as well as electro-magnetic properties [26–32]. In this work, Ni^{2+} in different ratios were substituted into Co^{2+} sites of cobalt phosphate octahydrate to improve the physical properties such as colour for using as ceramic pigment or as the catalyst due to the increasing thermal stability and surface area.

Transition metal phosphate hydrates have been extensively prepared to be precursors for anhydrous and pyrophosphate due to its capability to be transformed into various phosphate forms at elevated temperature via dehydration and polycondensation processes [33–40]. Recently, Viter and Nagornyi reported the synthesis of $(Ni_xCo_{1-x})_3(PO_4)_2 \cdot 8H_2O$ ($0 \leq x \leq 1$) by reacting a mixture of $CoSO_4$ and $NiSO_4$ solution with a Na_2HPO_4 solution at a particular (Co + Ni)/P molar ratio in the starting reagents of 3:2 (stoichiometric) at 90 °C, and the reaction duration of 1–5 days [3].

In this work, a series of binary cobalt nickel diphosphate octahydrates $Co_{3x}Ni_{3-3x}(PO_4)_2 \cdot 8H_2O$ ($x = 1$, 0.8, 0.6, 0.4, 0.2, and 0)

* Corresponding author. Materials Chemistry Research Unit, Department of Chemistry and Center for Innovation in Chemistry, Khon Kaen University, Khon Kaen 40002, Thailand. Tel.: +66 43 202222x12243; fax: +66 43 202373.
E-mail address: chanai@kku.ac.th (C. Danvirutai).

1293-2558/$ – see front matter © 2013 Elsevier Masson SAS. All rights reserved.
http://dx.doi.org/10.1016/j.solidstatesciences.2013.07.005

were prepared via simple and energy saving (70 °C for 24 h) method as compared with those reported in the literature [3]. The synthesized hydrates and their calcined products were characterized by using X-ray powder diffraction (XRD, Bruker AXS, Karlsruhe, Germany), Fourier transform infrared spectroscopy (FTIR, Perkin–Elmer spectrum GX FTIR/FT Raman spectrophotometer), thermogravimetry/differential thermogravimetric analysis/differential thermal analysis (TG/DTG/DTA, Perkin–Elmer Pyris Diamond) and atomic absorption spectrophotometry (AAS, Perkin–Elmer Analyst 100) techniques. Thermal behaviours of single and binary cobalt nickel diphosphate octahydrates were studied in details for the first time. Subsequently the morphology and surface data of the studied compounds were investigated using the scanning electron microscopy (SEM, LEO SEM VP1450) and Brunauer, Emmett and Teller (BET) method (Autosorb-1, Quanta Chrome Instrument).

2. Experimental

Single and binary cobalt nickel diphosphate octahydrates, $Co_{3x}Ni_{3-3x}(PO_4)_2\cdot 8H_2O$, where $x = 1$, 0.8, 0.6, 0.4, 0.2 and 0 were synthesized through the wet chemical reaction between $NiSO_4\cdot 6H_2O$, $CoSO_4\cdot 7H_2O$ and $Na_3PO_4\cdot 12H_2O$ solutions with various stoichiometric ratios of Ni/Co. The typical synthesis was performed by mixing 0.2 M $NiSO_4\cdot 6H_2O$ and 0.2 M $CoSO_4\cdot 7H_2O$ at each metal cation ratio, then 40 mL of 0.2 M $Na_3PO_4\cdot 12H_2O$ was added with the molar ratio of (Ni + Co)/P of 3:2 and the total volume of 100 mL. The suspension mixture was heated at 70 °C for 24 h. The particular precipitates were obtained and isolated by filtration, washed with DI water several times, dried at 100 °C and kept in a desiccator. The different colours of precipitates were obtained depending on the ratio of Ni/Co. The synthesized products were calcined at 700 and 900 °C for 4 h in air. The calcined products of hydrates were confirmed to be the corresponding anhydrous of nickel cobalt phosphates. The metal contents of $Co_{3x}Ni_{3-3x}(PO_4)_2\cdot 8H_2O$ ($x = 1$, 0.8, 0.6, 0.4, 0.2, and 0) were determined by AAS technique. The water contents in the synthesized hydrates were calculated from the TG/DTG/DTA data at the heating rate of 10 °C min^{-1} over the temperature range of 50–1000 °C in N_2 atmosphere. The water content was also determined by gravimetric method. The vibrational spectra of the studied compounds were recorded at room temperature in the wavenumber range of 4000–370 cm^{-1} with 32 scans and 4 cm^{-1} resolution using KBr press technique. The structure of the synthesized hydrates and the calcined products were studied by XRD technique using Cu K_α radiation ($\lambda = 0.15406$ nm) in the scanning 2θ angle range of 5–70°

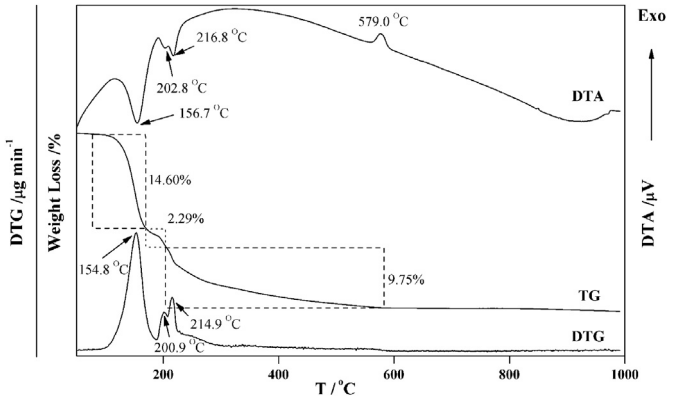

Fig. 1. TG/DTG/DTA curves of $Co_3(PO_4)_2\cdot 8H_2O$ at heating rate of 10 °C min^{-1} in N_2 atmosphere over the temperature range of 50–1000 °C.

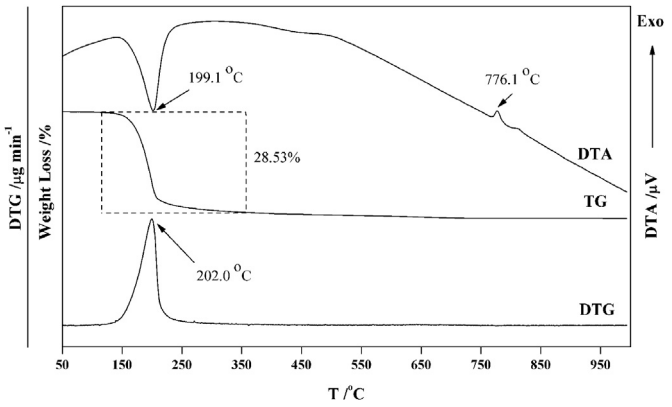

Fig. 2. TG/DTG/DTA curves of $Ni_3(PO_4)_2\cdot 8H_2O$ at heating rate of 10 °C min^{-1} in N_2 atmosphere over the temperature range of 50–1000 °C.

at the rate of 1° min^{-1}. The working voltage of instrument was 40 kV and the current was 40 mA. The lattice parameters and average crystallite sizes of these compounds were calculated from the XRD data. The Scherrer method was used to evaluate the crystallite size (i.e., $D = K\lambda/(\beta \cos\theta)$, where λ is wavelength of X-ray radiation, K is a constant taken as 0.89, θ is the diffraction angle and β is the full width at half-maximum (fwhm) [41]). The morphologies of the synthesized hydrates and their calcined products were studied by using the SEM technique with the mentioned instrument after gold coating. The surface area and pore size data of the anhydrous compounds were measured by BET method using N_2 adsorption at −190 °C.

3. Results and discussion

3.1. Chemical analysis

The water contents of the synthesized hydrates were determined by using TG/DTG/DTA and gravimetric methods, while the metal contents were confirmed by using AAS method.

TG/DTG/DTA curves of $Co_3(PO_4)_2\cdot 8H_2O$, $Ni_3(PO_4)_2\cdot 8H_2O$ and $Co_{3x}Ni_{3-3x}(PO_4)_2\cdot 8H_2O$ ($x = 0.8$, 0.6, 0.4 and 0.2) are illustrated in Figs. 1–3, respectively. The $Co_3(PO_4)_2\cdot 8H_2O$ exhibits three steps of the dehydration with the corresponding maxima DTG peaks at 154.8, 200.9, 214.9 °C, which agree well with DTA peaks at 156.7,

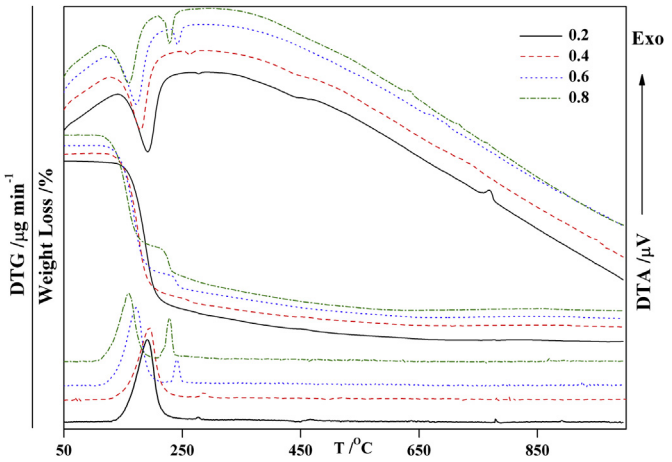

Fig. 3. TG/DTG/DTA curves of $Co_{3x}Ni_{3-3x}(PO_4)_2\cdot 8H_2O$ ($x = 0.8$, 0.6, 0.4 and 0.2) at heating rate of 10 °C min^{-1} in N_2 atmosphere over the temperature range of 50–1000 °C.

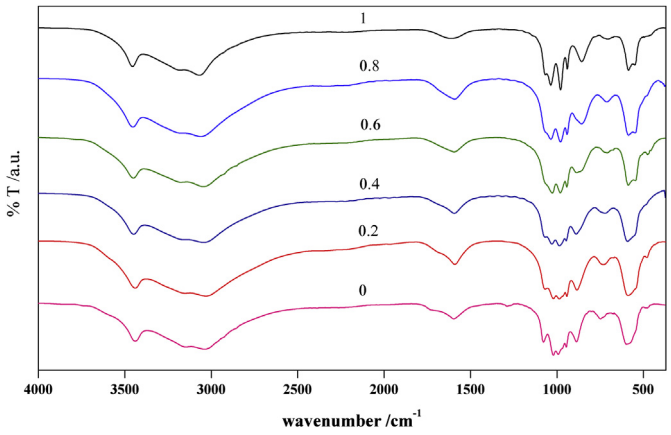

Fig. 4. FTIR spectra of $Co_{3x}Ni_{3-3x}(PO_4)_2{\cdot}8H_2O$, where $x = 1$, 0.8, 0.6, 0.4, 0.2, and 0.

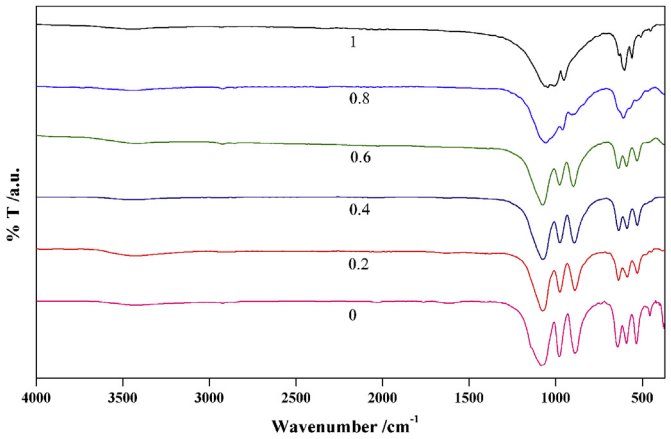

Fig. 6. FTIR spectra of calcined products of $Co_{3x}Ni_{3-3x}(PO_4)_2{\cdot}8H_2O$, where $x = 1$, 0.8, 0.6, 0.4, 0.2, and 0 at 900 °C in air atmosphere.

202.8 and 216.8 °C, respectively. Additional exothermal DTA peak at 579.0 °C was observed without weight loss and suggested to be due to the phase transition from low to high crystallinity [8]. The corresponding observed weight losses of three steps are 14.60% (~4 mol of H_2O), 2.29% (~1 mol of H_2O), and 9.75% (~3 mol of H_2O), which confirms the $Co_3(PO_4)_2{\cdot}8H_2O$ formula. The thermal decomposition reactions can be suggested as the following:

$$Co_3(PO_4)_2{\cdot}8H_2O \overset{100-180\ ^\circ C}{\rightarrow} Co_3(PO_4)_2{\cdot}4H_2O + 4H_2O \quad (1)$$

$$Co_3(PO_4)_2{\cdot}4H_2O \overset{180-200\ ^\circ C}{\rightarrow} Co_3(PO_4)_2{\cdot}3H_2O + H_2O \quad (2)$$

$$Co_3(PO_4)_2{\cdot}3H_2O \overset{200-600\ ^\circ C}{\rightarrow} Co_3(PO_4)_2 + 3H_2O \quad (3)$$

The elimination of water of crystallization at three different temperature maxima revealed that there are three groups of hydrogen bonding species of different strengths. The weight loss in the temperature range of 250–600 °C can be referred to as the loss of coordinated link water molecules [42].

In contrast, the TG/DTG/DTA curve of $Ni_3(PO_4)_2{\cdot}8H_2O$ (Fig. 2) shows only one dehydration step with the maximum temperature DTG peak at 199.9 °C, which agrees with the DTA peak at 201.7 °C. The exothermal DTA peak at 776.1 °C is suggested to be similar to the previous case due to the phase transition from low to high crystallinity. The observed total weight loss over the temperature range of 150–250 °C is 28.53% (8.1 mol of water of crystallization), which is consistent with the theoretical weight loss (28.23%) confirming 8 mol of water of crystallization in the hydrate formula. The thermal decomposition reaction can be suggested as follows:

$$Ni_3(PO_4)_2{\cdot}8H_2O \overset{150-250\ ^\circ C}{\rightarrow} Ni_3(PO_4)_2 + 8H_2O \quad (4)$$

In the case of binary cobalt nickel diphosphate octahydrates ($Co_{3x}Ni_{3-3x}(PO_4)_2{\cdot}8H_2O$; $x = 0.8$, 0.6, 0.4 and 0.2), TG/DTG/DTA curves are illustrated in Fig. 3. The TG/DTG/DTA curve of $Co_{2.4}Ni_{0.6}(PO_4)_2{\cdot}8H_2O$ ($x = 0.8$) shows the same character as $Co_3(PO_4)_2{\cdot}8H_2O$ (Fig. 1), which illustrates three decomposition steps. In contrast, $Co_{0.6}Ni_{2.4}(PO_4)_2{\cdot}8H_2O$ ($x = 0.2$) shows the same character as $Ni_3(PO_4)_2{\cdot}8H_2O$ (Fig. 2), which illustrates only one decomposition step. However, the TG/DTG/DTA curves of $Co_{1.8}Ni_{1.2}(PO_4)_2{\cdot}8H_2O$ ($x = 0.6$) and $Co_{1.2}Ni_{1.8}(PO_4)_2{\cdot}8H_2O$ ($x = 0.4$) show the intermediate behaviour between two single cation compounds in such a way that, two decomposition steps were observed. The dehydration temperature of binary cobalt nickel diphosphate octahydrates occurred at higher temperature, when the nickel contents were increased. The water contents in the synthesized phosphate hydrates from gravimetric method agree well with result from TG data. The results from gravimetric

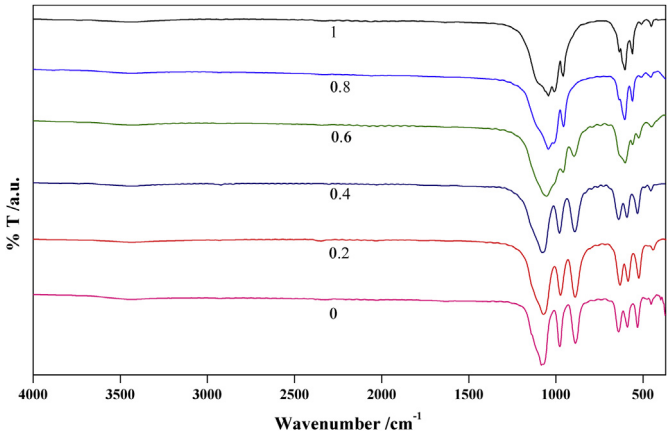

Fig. 5. FTIR spectra of calcined products of $Co_{3x}Ni_{3-3x}(PO_4)_2{\cdot}8H_2O$, where $x = 1$, 0.8, 0.6, 0.4, 0.2, and 0 at 700 °C in air atmosphere.

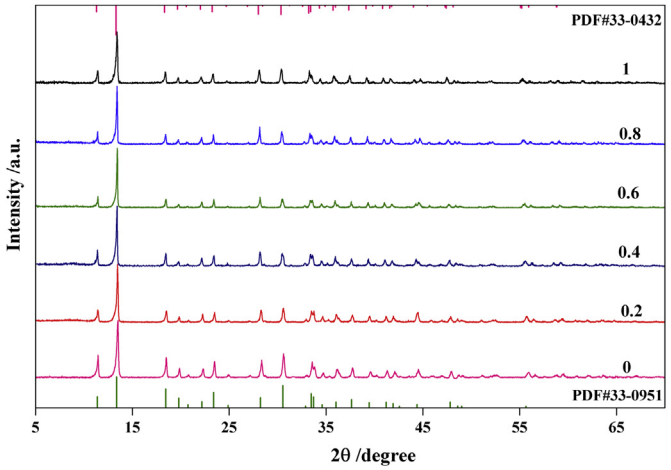

Fig. 7. XRD patterns of synthesized hydrates $Co_{3x}Ni_{3-3x}(PO_4)_2{\cdot}8H_2O$, where $x = 1$, 0.8, 0.6, 0.4, 0.2 and 0.

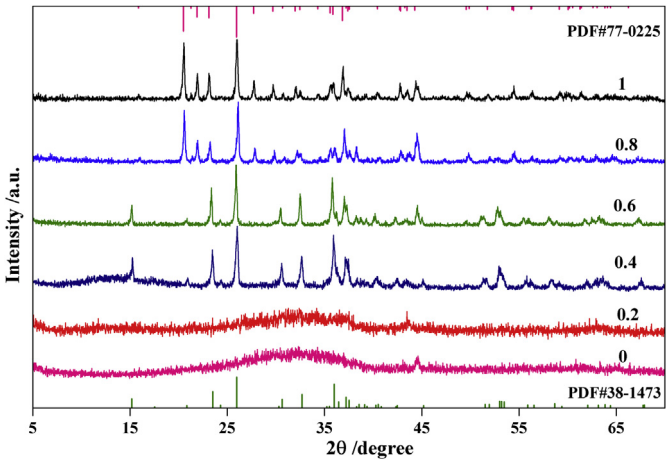

Fig. 8. XRD patterns of calcined products of $Co_{3x}Ni_{3-3x}(PO_4)_2{\cdot}8H_2O$, where $x = 1$, 0.8, 0.6, 0.4, 0.2 and 0, at 700 °C in air atmosphere.

analysis for $Co_{3x}Ni_{3-3x}(PO_4)_2{\cdot}8H_2O$ ($x = 1$, 0.8, 0.6, 0.4, 0.2, and 0) also agree well with TG results.

3.2. Vibrational spectroscopic study

Vibrational spectroscopic study of the synthesized phosphates was carried out in the range of 4000–370 cm^{-1}. The FTIR spectra of $Co_{3x}Ni_{3-3x}(PO_4)_2{\cdot}8H_2O$, ($x = 1$, 0.8, 0.6, 0.4, 0.2, and 0) and their calcined products at 700 and 900 °C are demonstrated in Figs. 4–6, respectively. The vibrational bands of $Ni_3(PO_4)_2{\cdot}8H_2O$ (Fig. 4) in the region of 3182–3038 cm^{-1} are assigned to $\nu_1(A_1)H_2O$, whereas the bands at about 3438 cm^{-1} is attributed to $\nu_3(B_2)H_2O$. The bending mode of water, $\nu_2(A_1)H_2O$, was observed at around 1596 cm^{-1}. The splitting of $\nu_2(A_1)H_2O$ bands in $Ni_3(PO_4)_2{\cdot}8H_2O$ indicates that the molecules of water of crystallization locate at more than one different site groups or there are more than one crystallographic distinct water molecules. The vibrational (hindered rotational) modes of water observed at 746 cm^{-1} are attributed to rocking mode (ρ_r) [43,44]. The observed bands in the ranges of 1076–990 cm^{-1}, 966–884 cm^{-1}, 596–543 cm^{-1} and 474 cm^{-1} are assigned to $\nu_3(F_2)PO_4^{3-}$, $\nu_1(A_1)PO_4^{3-}$, $\nu_4(F_2)PO_4^{3-}$ and $\nu_2(E)PO_4^{3-}$, respectively. In the case of calcined product at 700 °C of $Ni_3(PO_4)_2{\cdot}8H_2O$, the corresponding bands were observed in the ranges of 1140–1068 cm^{-1}, 976–887 cm^{-1}, 640–531 cm^{-1} and 453 cm^{-1}, respectively (Fig. 4). The splitting of triply degenerate mode $\nu_3(F_2)$ of PO_4^{3-} is interpreted to be due to the PO_4^{3-} ions locating at the site symmetry lower than T_d or locate at more than one different sites. The vibrational bands at 3454 cm^{-1} of $Co_3(PO_4)_2{\cdot}8H_2O$ (Fig. 4) is assigned to asymmetric stretching $\nu_3(B_2)H_2O$ and the broad bands in the region of 3185–3068 cm^{-1} are attributed to hydrogen bonded $\nu_1(A_1)H_2O$. The bending mode of water, $\nu_2(A_1)H_2O$, was observed at 1611 cm^{-1}. The vibrational stretching bands of water in $Co_3(PO_4)_2{\cdot}8H_2O$ occurred at higher wavenumbers than that of $Ni_3(PO_4)_2{\cdot}8H_2O$. This can be interpreted

Table 1
Lattice parameters and average crystallite sizes of synthesized hydrates and their calcined products calculated from XRD data.

Compounds		a/Å	b/Å	c/Å	β/°	Average crystallite sizes/nm
$Co_3(PO_4)_2{\cdot}8H_2O$	PDF # 33-0432	9.926	13.33	4.678	102.31	–
	This work	9.916	13.33	4.679	102.30	68.2 ± 2
	PDF-this work	0.010	0.00	−0.001	0.01	–
$Co_3(PO_4)_2$	PDF # 77-0225	7.556	8.371	5.064	94.050	–
	This work	7.559	8.369	5.067	94.074	40.5 ± 4
	PDF-this work	−0.003	0.002	−0.003	−0.024	–
$Ni_3(PO_4)_2{\cdot}8H_2O$	PDF # 33-0951	9.846	13.20	4.634	102.27	–
	This work	9.845	13.16	4.634	102.31	63.2 ± 8
	PDF-this work	0.001	0.004	0.000	−0.04	–
$Ni_3(PO_4)_2$	PDF # 38-1473	10.09	4.698	5.827	91.138	–
	This work	10.11	4.699	5.828	90.869	58.2 ± 10
	PDF-this work	−0.02	−0.001	−0.001	0.270	–
$Co_{2.4}Ni_{0.6}(PO_4)_2{\cdot}8H_2O$	PDF #	–	–	–	–	–
	This work	9.979	13.56	4.646	101.22	102.4 ± 3
$Co_{2.4}Ni_{0.6}(PO_4)_2$	PDF #	–	–	–	–	–
	This work	11.167	9.672	10.095	80.98	73.4 ± 16
$Co_{1.8}Ni_{1.2}(PO_4)_2{\cdot}8H_2O$	PDF #	–	–	–	–	–
	This work	9.794	13.62	4.748	103.28	99.9 ± 54
$Co_{1.8}Ni_{1.2}(PO_4)_2$	PDF #	–	–	–	–	–
	This work	11.474	5.485	6.819	84.75	88.5 ± 0.4
$Co_{1.2}Ni_{1.8}(PO_4)_2{\cdot}8H_2O$	PDF #	–	–	–	–	–
	This work	9.708	13.62	4.746	103.68	78.1 ± 49
$Co_{1.2}Ni_{1.8}(PO_4)_2$	PDF #	–	–	–	–	–
	This work	10.208	4.718	5.8870	90.83	70.3 ± 12
$Co_{0.6}Ni_{2.4}(PO_4)_2{\cdot}8H_2O$	PDF #	–	–	–	–	–
	This work	9.863	13.22	4.642	102.34	62.5 ± 15
$Co_{0.6}Ni_{2.4}(PO_4)_2$	PDF #	–	–	–	–	–
	This work	10.154	4.711	5.852	91.02	58.4 ± 18

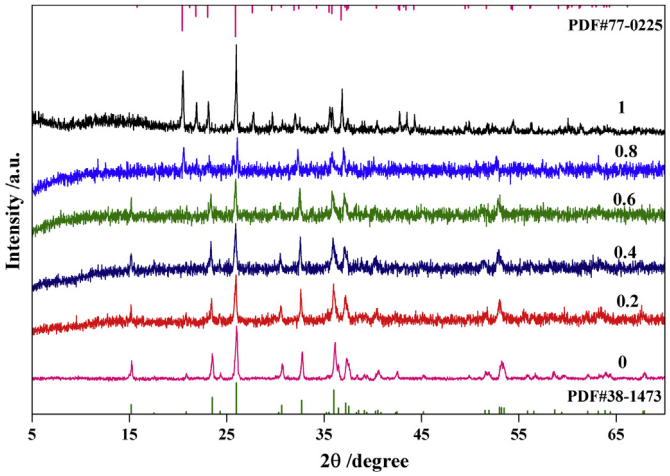

Fig. 9. XRD patterns of calcined products of $Co_{3x}Ni_{3-3x}(PO_4)_2{\cdot}8H_2O$, where $x = 1$, 0.8, 0.6, 0.4, 0.2 and 0, at 900 °C in air atmosphere.

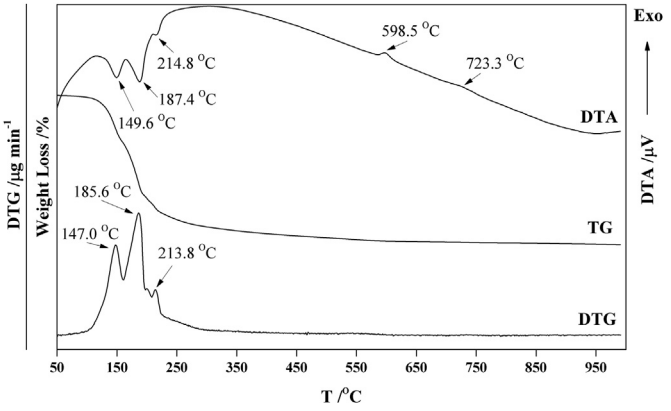

Fig. 10. TG/DTG/DTA curves of the mixture between 0.6 mol of $Co_3(PO_4)_2{\cdot}8H_2O$ to 0.4 mol of $Ni_3(PO_4)_2{\cdot}8H_2O$ at heating rate of 10 °C min^{-1} in N_2 atmosphere over the temperature range of 50–1000 °C.

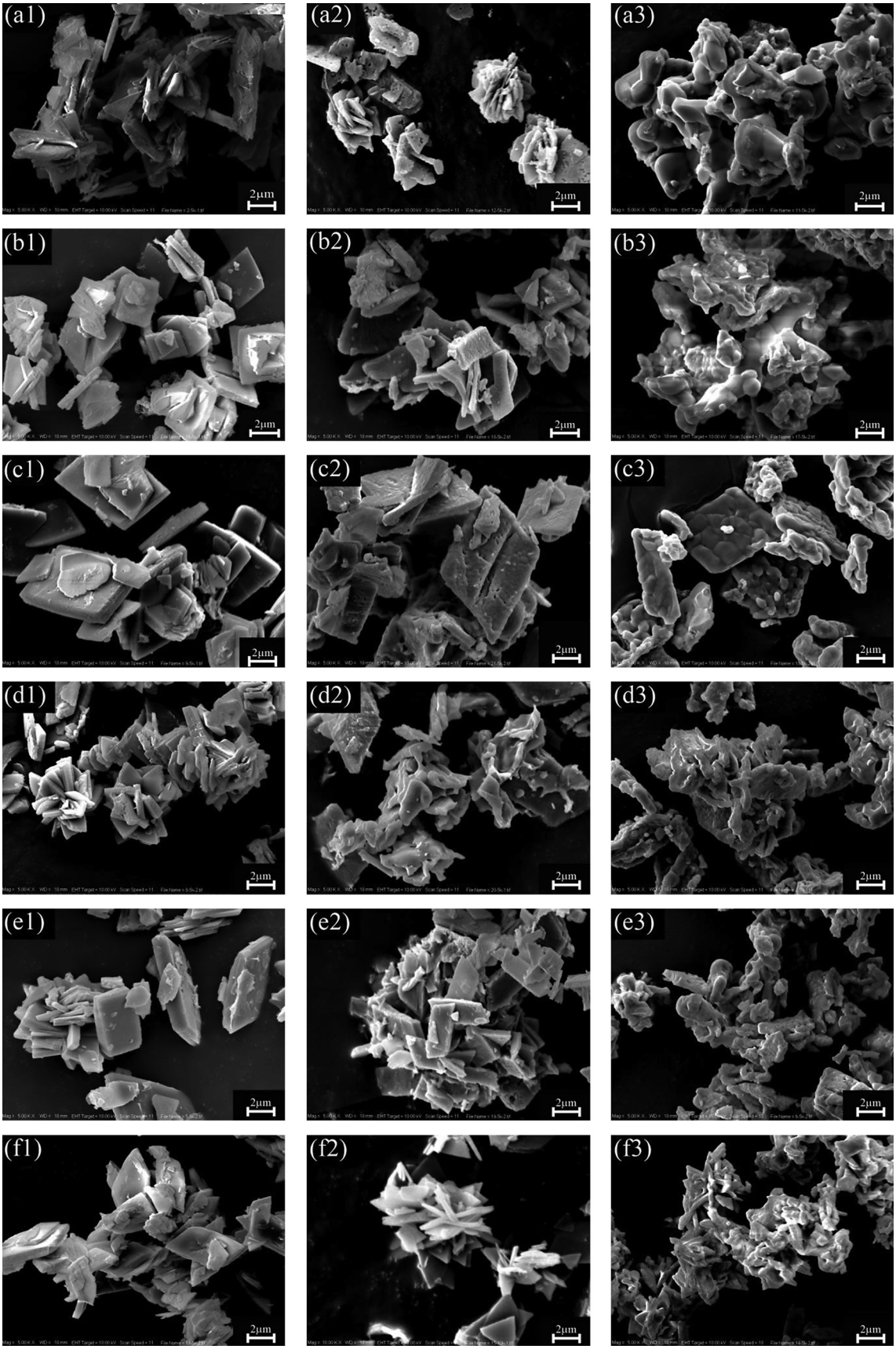

Fig. 11. SEM micrographs of synthesized $Co_{3x}Ni_{3-3x}(PO_4)_2 \cdot 8H_2O$ (1), $x = 1$ (a), 0.8 (b), 0.6 (c), 0.4 (d), 0.2 (e), and 0 (f), and their calcined products at 700 °C (2) and 900 °C (3) in air atmosphere for 4 h.

to be due to the smaller radius of Ni^{2+} than Co^{2+} providing high surface charge density and hence influencing additional effect on hydrogen bonding. Therefore, the coordinate covalent bonding interaction between Ni^{2+} and OH_2 should be stronger than the interaction between Co^{2+} and OH_2, consequently strengthens the H-bonding. The observed bands at 1066–977 cm^{-1}, 938 cm^{-1}, 584–546 cm^{-1} and 466 cm^{-1} are assigned to $\nu_3(F_2)PO_4^{3-}$, $\nu_1(A_1)PO_4^{3-}$, $\nu_4(F_2)PO_4^{3-}$ and $\nu_2(E)PO_4^{3-}$, respectively. The vibrational modes of water observed at 703 cm^{-1} are attributed to rocking mode (ρ_r) [43]. The observed bands around of 1103–1009 cm^{-1}, 958 cm^{-1} and 635–509 cm^{-1}, and 452 cm^{-1} of calcined products at 900 °C of $Co_3(PO_4)_2\cdot 8H_2O$ (Fig. 5) are assigned to $\nu_3(F_2)PO_4^{3-}$, $\nu_1(A_1)PO_4^{3-}$, $\nu_4(F_2)PO_4^{3-}$ and $\nu_2(E)PO_4^{3-}$, respectively. The FTIR spectrum of binary cobalt nickel diphosphate octahydrate for $x = 0.8$ (Fig. 4) exhibits the same character as the single cobalt phosphate octahydrate, while the spectrum of binary cobalt nickel diphosphate octahydrate for $x = 0.2$ (Fig. 4) is similar to the spectrum of single nickel diphosphate octahydrate. However, the x value of 0.4 and 0.6 illustrate mixed spectral behaviours between the mentioned two single metal phosphates.

3.3. Structural analysis

The structures, lattice parameters, and crystallite sizes of the synthesized hydrates and their calcined products at 700 and 900 °C in air atmosphere were determined from XRD data as demonstrated in Figs. 7–9, respectively. The lattice parameters calculated using the computer program and the crystallite sizes evaluated from Scherrer equation are tabulated in Table 1. $Co_3(PO_4)_2\cdot 8H_2O$ and $Ni_3(PO_4)_2\cdot 8H_2O$ are isostructure and crystallize in monoclinic system with the space group I2m or C_{2h}^3 (12), $Z = 2$. The lattice parameters of $Co_3(PO_4)_2\cdot 8H_2O$ agree well with the PDF # 33-0432 as well as those of $Ni_3(PO_4)_2\cdot 8H_2O$ corresponding to the PDF # 33-0951 (Table 1). The anhydrous cobalt and nickel phosphates are isostructure with their hydrate precursors. They crystallize in monoclinic system in the space group $P2_1/a$ or C_{2h}^5 (14), $Z = 2$. The lattice parameters of $Co_3(PO_4)_2$ agree well with the PDF # 77-0225, while those of $Ni_3(PO_4)_2$ correspond to the PDF # 38-1473 (Table 1). In the case of binary tri(cobalt nickel) diphosphate octahydrates, the XRD pattern of $Co_{0.6}Ni_{2.4}(PO_4)_2\cdot 8H_2O$ (Fig. 7) shows the same character as $Ni_3(PO_4)_2\cdot 8H_2O$ (notice plane 350), while the pattern of $Co_{2.4}Ni_{0.6}(PO_4)_2\cdot 8H_2O$ exhibits the same character as $Co_3(PO_4)_2\cdot 8H_2O$ (notice plane 350 and −161). The XRD patterns of $Co_{1.2}Ni_{1.8}(PO_4)_2\cdot 8H_2O$ and $Co_{1.8}Ni_{1.2}(PO_4)_2\cdot 8H_2O$ reveals the same character as both $Co_3(PO_4)_2$ and $Ni_3(PO_4)_2$. The lattice parameters of the binary cation compounds lie between those of the single cation compounds. The average crystallite sizes of binary tri(cobalt nickel) diphosphate octahydrates tend to be larger as the molar ratios of cobalt increase. In the cases of the calcined products at 700 °C in air atmosphere for 4 h, the XRD results (Fig. 8) show that the crystallinity of $Co_{0.6}Ni_{2.4}(PO_4)_2$ and $Ni_3(PO_4)_2$ are low, while the XRD patterns of their calcined products at 900 °C of $Co_{0.6}Ni_{2.4}(PO_4)_2$ and $Ni_3(PO_4)_2$ (Fig. 9) show higher crystallinity. The crystallinity of $Co_{3x}Ni_{3-3x}(PO_4)_2$ for $x = 1$, 0.8, 0.6, and 0.4 were obtained at 700 °C, whereas the crystallinity of the compounds with $x = 0.2$ and 0 were obtained at 900 °C. The XRD patterns and the lattice parameters of $Co_{3x}Ni_{3-3x}(PO_4)_2$ for $x = 0.6$, 0.4, and 0.2 exhibit are close to that of the anhydrous $Ni_3(PO_4)_2$, while for $x = 0.8$ showing the same character as that of the anhydrous $Co_3(PO_4)_2$. The average crystallite sizes of the anhydrous products are smaller than that of the hydrate precursors. The sharp peaks of XRD patterns of binary cobalt nickel diphosphate octahydrates can confirm the single phase with high crystallinity. Furthermore, the difference between TG/DTG/DTA curves of $Co_{1.8}Ni_{1.2}(PO_4)_2\cdot 8H_2O$ (Fig. 3) compared with that of the prepared mixture between two phases of 0.6 mol of $Co_3(PO_4)_2\cdot 8H_2O$ and 0.4 mol of $Ni_3(PO_4)_2\cdot 8H_2O$ (Fig. 10) are additional proof for the confirmation of the single phase of binary cobalt nickel diphosphate octahydrates. The TG/DTG/DTA curves of the mixture of 0.6 mol of $Co_3(PO_4)_2\cdot 8H_2O$ and 0.4 mol of $Ni_3(PO_4)_2\cdot 8H_2O$ (Fig. 9) show four maxima DTG peaks, while the thermogram of $Co_{1.8}Ni_{1.2}(PO_4)_2\cdot 8H_2O$ (Fig. 3) exhibits two DTG peaks, which appear at higher temperatures than the previously mentioned cases. Additionally, the thermogram of the prepared mixture of two single phases of 0.6 mol of $Co_3(PO_4)_2\cdot 8H_2O$ and 0.4 mol of $Ni_3(PO_4)_2\cdot 8H_2O$ shows two exothermic DTA peaks, while only one exothermic DTA peak is observed in the thermogram of $Co_{1.8}Ni_{1.2}(PO_4)_2\cdot 8H_2O$.

3.4. Morphology study

The SEM micrographs of $Co_{3x}Ni_{3-3x}(PO_4)_2\cdot 8H_2O$ ($x = 1$, 0.8, 0.6, 0.4, 0.2, and 0) and their calcined products at 700 and 900 °C in air atmosphere are shown in Fig. 11a–f. The morphologies of synthesized single nickel and cobalt phosphate octahydrates (Fig. 11a1 and f1, respectively) show the same morphologies, which exhibit thin plate. The small plate particles have the width and length of about 800 nm and 2000 nm, while the large ones are of about 1000 nm and 3000 nm with thickness of ~200–300 nm. The particle shapes of their calcined products at 700 and 900 °C in air atmosphere exhibited the smaller size than the synthetic hydrate. The mixed metal system (Fig. 11b–e) shows the same feature as single metal system, but the plate particles have various sizes. The small particles have a width and length of about 800 nm and 1000 nm. The large plate particles have a width, length and thickness of about 1000, 2000 and 500–1000 nm, respectively. Similarly, their calcined products of mixed metal system at 700 °C and 900 °C (Fig. 11b–e) also show the small thin plate particles with smaller size than the synthetic hydrates.

3.5. BET surface properties

The surface area and pore size data of the anhydrous compounds were measured using nitrogen adsorption based on BET method at −190 °C as presented in Table 2. The surface areas of both single and binary tri(cobalt nickel) diphosphate anhydrous forms are close to each other (Table 2), whereas $Co_{2.4}Ni_{0.6}(PO_4)_2$ ($x = 0.8$) shows the highest surface area (10.57 $m^2\ g^{-1}$), which is nearly double as compared with those of the single metal and other ratios of metal compounds. The binary mixture of Co:Ni of 2.4:0.6 is suggested to be the best ratio to produce the highest surface area compound that can improve the catalytic activity. From the average pore diameters measurement, the mesopores were observed in all studied compounds (Table 2). The smallest pore diameter of $Co_{2.4}Ni_{0.6}(PO_4)_2$ is consistent with the highest surface area. Thus, the pore volume of this binary metal ratio is highest among all of them. The surface properties of the studied compounds are reported for the first time.

Table 2
Surface area, average pore diameter and total pore volume of anhydrous $Co_{3x}Ni_{3-3x}(PO_4)_2$.

Compounds	Surface area/$m^2\ g^{-1}$	Average pore diameter/Å	Total pore volume/$cm^3\ g^{-1}$
$Co_3(PO_4)_2$	4.040	96.19	9.717×10^{-3}
$Co_{2.4}Ni_{0.6}(PO_4)_2$	10.57	50.77	1.342×10^{-2}
$Co_{1.8}Ni_{1.2}(PO_4)_2$	5.078	90.23	1.145×10^{-2}
$Co_{1.2}Ni_{1.8}(PO_4)_2$	2.940	169.5	1.246×10^{-2}
$Co_{0.6}Ni_{2.4}(PO_4)_2$	3.269	157.2	1.285×10^{-2}
$Ni_3(PO_4)_2$	3.418	167.5	1.431×10^{-2}

4. Conclusion

$Co_{3x}Ni_{3-3x}(PO_4)_2 \cdot 8H_2O$ (x = 1, 0.8, 0.6, 0.4, 0.2, and 0) were successfully synthesized by the simple and energy saving route compared with those reported in the literature. The results from AAS technique confirmed the contents of cobalt and nickel in synthesized hydrates, which agree well with the required formula. The water contents of the synthesized hydrates were determined by using TG/DTG/DTA and gravimetric methods. The sharp peaks of XRD patterns confirm the single phase of $Co_{3x}Ni_{3-3x}(PO_4)_2 \cdot 8H_2O$ (x = 1, 0.8, 0.6, 0.4, 0.2, and 0). Besides, the difference between TG/DTG/DTA thermograms of $Co_{1.8}Ni_{1.2}(PO_4)_2 \cdot 8H_2O$ (x = 0.6) and the mixture of two single phases of 0.6 mol of $Co_3(PO_4)_2 \cdot 8H_2O$ to 0.4 mol of $Ni_3(PO_4)_2 \cdot 8H_2O$ is the additional proof for the existence of the single phase of binary tri(cobalt nickel) diphosphate octahydrates. The thermal behaviours of the studied systems are reported for the first time. From the surface data measurement, the mesopores were observed in all studied compounds and the anhydrous binary metal phosphate at x = 0.8 ($Co_{2.4}Ni_{0.6}(PO_4)_2$) showed the highest surface area (10.57 $m^2\ g^{-1}$), which was about ten times of the hydrate precursor. The morphologies and surface properties of the synthesized hydrates and their calcined products are reported for further applications in the area of catalysis. The FTIR spectra of the studied compounds were recorded and assigned.

Acknowledgement

The financial support from Khon Kaen University through the Materials Chemistry Research Unit, Center for Innovation in Chemistry (PERCH-CIC), Ministry of Education, the Higher Education Research Promotion and National Research University Project of Thailand, Office of Higher Education Commission, through the Advanced Functional Materials Cluster of Khon Kaen University, is gratefully acknowledged.

References

[1] N.N. Prokopchuk, V.A. Kopilevich, L.V. Voitenko, Zh. Prikl. Khim. 81 (2007) 399–404.
[2] S. Mesguer, M.A. Tena, C. Gargori, R. Galindo, J.A. Badenes, M. Llusar, G. Monrós, Ceram. Int. 34 (2008) 1431–1438.
[3] V.N. Viter, P.G. Nagornyi, Zh. Prikl. Khim. 82 (6) (2009) 881–885.
[4] M. Trojan, Dyes Pigm. 13 (1) (1990) 1–10.
[5] S. Mesguer, M.A. Tena, C. Gargori, J.A. Badenes, M. Llusar, G. Monrós, Ceram. Int. 33 (2007) 843–849.
[6] I.C. Marcu, I. Sandulescu, J.M.M. Millet, Appl. Catal. A Gen. 277 (2002) 309–320.
[7] A. Benarafa, M. Kacimi, G. Coudurier, M. Ziyad, Appl. Catal. A Gen. 196 (2000) 25–35.
[8] M.A. Aramendía, V. Borau, C. Jiménez, J.M. Marinas, F.J. Romero, J. Colloid Interface Sci. 217 (1999) 288–298.
[9] A. Aaddane, M. Kacimi, M. Ziyad, Catal. Lett. 73 (2001) 47–53.
[10] R.D.A. Gaasbeek, H.G. Toonen, R.J. van Heerwaarden, P. Buma, Biomaterials 26 (2005) 6713–6719.
[11] J.M. Rojo, J.L. Mesa, J.L. Pizarro, L. Lezama, M.I. Arriortua, T. Rojo, Mater. Res. Bull. 31 (1996) 925–934.
[12] J. Escobal, J.L. Pizarro, J.L. Mesa, J.M. Rojo, B. Bazan, M.I. Arriortua, T. Rojo, J. Solid State Chem. 178 (2005) 2626–2634.
[13] O. Pawlig, R. Trettin, Mater. Res. Bull. 34 (1998) 1959–1966.
[14] C.E. Bamberger, J. Am. Ceram. Soc. 81 (1) (1998) 252–256.
[15] G.S. Kumar, E.K. Girija, A. Thamizhavel, Y. Yokogawa, N. Kalkura, J. Colloid Interface Sci. 349 (2010) 56–62.
[16] R.Z. LeGeros, Chem. Rev. 108 (2008) 4742–4753.
[17] W. Paul, C.P. Sharma, J. Mater. Sci. Mater. Med. 10 (1999) 383–388.
[18] V. Stanić, S. Dimitrijević, J. Antić-Stanković, M. Mitić, B. Jokić, I.B. Plećaš, S. Raičevi&cacute, Appl. Surf. Sci. 256 (2010) 6083–6089.
[19] M.B. Sorensen, R.G. Hazell, J. Chevallier, N. Pind, T.R. Jensen, Microporous Mesoporous Mater. 84 (2005) 144–152.
[20] S.N. Le, A. Navrotsky, J. Solid State Chem. 181 (2008) 20–29.
[21] J.H. Jun, K.S. Jeong, T.J. Lee, S.J. Kong, T.H. Lim, S.W. Nam, S.A. Hong, K.J. Yoon, Korean J. Chem. Eng. 21 (1) (2004) 140–146.
[22] M. Bahidsky, M. Hronce, Catal. Today 99 (2005) 187–192.
[23] J.H. Jun, T.J. Lee, S.W. Nam, S.A. Hong, K.J. Yoon, J. Catal. 211 (2004) 178–190.
[24] V.N. Viter, Zh. Prikl. Khim. 82 (12) (2009) 1952–1956.
[25] V.N. Viter, P.G. Nagornyi, Zh. Prikl. Khim. 42 (4) (2006) 460–463.
[26] M. Trojan, Dyes Pigm. 12 (4) (1990) 307–318.
[27] J.W. Fergus, J. Power Sources 195 (2010) 939–954.
[28] D. Wang, H. Li, S. Shi, X. Huang, L. Chen, Electrochim. Acta 50 (2005) 2955–2958.
[29] A.Y. Shenouda, H.K. Liu, J. Alloys Compd. 477 (2009) 498–503.
[30] A. Goñi, L. Lezama, G.E. Braberis, J.L. Pizarro, M.I. Arriortua, T. Rojo, J. Magn. Magn. Mater. 164 (1996) 251–255.
[31] D. Wang, Z. Wang, X. Huang, L. Chen, J. Power Sources 146 (2005) 580–583.
[32] Y.C. Chen, J.M. Chen, C.H. Hsu, J.W. Yeh, H.C. Shih, Y.S. Cheng, H.S. Sheu, J. Power Sources 189 (2009) 790–793.
[33] B. Boonchom, Int. J. Thermophys. 31 (2010) 416–429.
[34] B. Boonchom, S. Youngme, S. Maensiri, C. Danvirutai, J. Alloys Compd. 454 (2008) 78–82.
[35] C. Danvirutai, B. Boonchom, S. Youngme, J. Alloys Compd. 457 (2008) 75–80.
[36] B. Boonchom, C. Danvirutai, J. Chem. Eng. Data 54 (4) (2009) 1225–1230.
[37] B. Boonchom, C. Danvirutai, S. Maensiri, Mater. Chem. Phys. 109 (2008) 404–410.
[38] P. Noisong, C. Danvirutai, B. Boonchom, J. Chem. Eng. Data 54 (2009) 871–875.
[39] P. Noisong, C. Danvirutai, J. Chem. Eng. Data 49 (2010) 3146–3151.
[40] B. Boonchom, S. Youngme, T. Srithanyaratana, C. Danvirutai, J. Therm. Anal. Calorim. 91 (2) (2008) 511–516.
[41] B.D. Cullity, Elements of X-ray Diffraction, second ed., Addison-Wesley Publishing, New York, 1997.
[42] B. Boonchom, C. Danvirutai, Ind. Eng. Chem. Res. 46 (2007) 9071–9076.
[43] H.D. Lutz, Struct. Bonding 69 (1988) 97.
[44] B. Boonchom, S. Maensiri, S. Youngme, C. Danvirutai, Solid State Sci. 11 (2009) 485–490.